

**Polarized-neutron-diffraction study of the magnetization density in hexagonal  $Y_2Fe_{17}$** 

O. Moze

*Dipartimento di Fisica, Università degli Studi di Parma, Via delle Scienze, 43100 Parma, Italy*

R. Caciuffo

*Dipartimento di Scienze dei Materiali e della Terra, Università degli Studi di Ancona, Via Breccie Bianche, 60131 Ancona, Italy*

B. Gillon

*Laboratoire Léon Brillouin, Centre d'Etudes Nucléaires, de Saclay, 91191, Gif-sur-Yvette, France*

G. Calestani

*Dipartimento di Chimica Fisica ed Inorganica, Università degli Studi di Bologna, Viale del Risorgimento 4, 40136 Bologna, Italy*

F. E. Kayzel and J. J. M. Franse

*Van der Waals-Zeeman Laboratorium, Universiteit van Amsterdam, Valckenierstraat 65-67, 1018 XE Amsterdam, The Netherlands*

(Received 10 March 1994; revised manuscript received 12 May 1994)

X-ray- and polarized-neutron-diffraction measurements have been carried out on a single crystal of hexagonal  $Y_2Fe_{17}$  in order to determine the details of the structural disorder and local-Fe-moment distribution. The crystal structure, as determined by x-ray diffraction, indicates a disordered variant of the  $Th_2Ni_{17}$  structure with formation of dumbbell Fe sites around Y sites  $2b$  and  $2c$ . These act to induce weak distortions on the nearby  $12k$  and  $12j$  Fe sites. For this particular crystal, with a refined stoichiometry of  $Y_2Fe_{17.3}$ , only the  $12j$  Fe site was found to decompose into two subsites. The magnetization density has been measured by polarized-neutron diffraction and fitted to a multipole model of the Fe moments. The calculated Fe magnetic moments are in good agreement with recent electronic band-structure calculations.

**I. INTRODUCTION**

Hexagonal rare-earth-transition-metal intermetallics, which crystallize in the  $Th_2Ni_{17}$  structure ( $P6_3/mmm$ ), are well-known prototypes of high-energy product permanent magnets. The small RE (rare-earth)-transition-metal ratio, large spontaneous magnetization, and high Curie temperatures all point to extremely favorable circumstances for applications. The contribution of the  $3d$  sublattice to magnetic properties such as the spontaneous magnetization and magnetocrystalline anisotropy is not as well understood as that of the RE atoms. This is due to the itinerant nature of the  $3d$  electrons and only recently have band-structure calculations advanced to the point where, for instance, the calculated magnetic moments in important intermetallics such as rhombohedral ( $R\bar{3}m$ , 19 atoms/unit cell) and hexagonal ( $P6_3/mmm$ , 38 atoms/unit cell) forms of  $Y_2Fe_{17}$  are in approximate agreement with available experimental data.<sup>1-4</sup> Yttrium compounds are ideal for this purpose since the supposed nonmagnetic Y atom is, for all intents and purposes, chemically similar to the trivalent RE atom. It has been assumed in the past that the magnetic moment at the Y site is zero, but both calculations,<sup>5</sup> pressure-dependent magnetization and measurements of the hyperfine field at the Y site, show that a moment of approximately  $0.4\mu_B$

coupled antiparallel to the Fe moment exists in  $YFe_2$ .<sup>6,7</sup>

Both rhombohedral and hexagonal forms of  $Y_2Fe_{17}$  compounds have attracted considerable interest since the magnetic properties can be enhanced by introduction of interstitial  $N$  (Refs. 8 and 9) with a corresponding increase in the unit cell volume of up to 8%, a change in the Curie temperature from 330 K to 700 K, with an associated increase in the saturation magnetization of up to 100%. Local magnetic moments at the various Fe and Y sites have been calculated on the basis of numerous and detailed electronic band-structure calculations<sup>10-17</sup> for both rhombohedral and hexagonal forms of  $Y_2Fe_{17}$ . The local environments of the Fe atoms in both these structures are very similar and local moments ranging from  $1.5$  up to  $2.5\mu_B$  are obtained. The magnetism of the hexagonal form of  $Y_2Fe_{17}$  has been exhaustively investigated by a large variety of experimental techniques and this system has been classified as an example of a weak ferromagnet. The following bulk magnetic properties have been reported: (a) a ferromagnetic Curie point of 324 K, which can reach up to 386 K for off-stoichiometric compounds, (b) a saturation magnetization at 4.2 K of  $35.2\mu_B$  per formula unit, (c) an anomalous thermal expansion below the ferromagnetic ordering temperature, (d) a large volume magnetostriction, and (e) a large pressure dependence of the Curie

point.<sup>18–20</sup> Previous unpolarized-neutron-diffraction investigations of the hexagonal modification indicate a collinear easy-plane magnetic structure.<sup>21</sup> The system always retains a planar anisotropy even with an excess Y composition.<sup>22</sup> The details of the magnetic anisotropy at low and intermediate temperatures have been studied in great detail with single crystalline materials.<sup>23–25</sup> Magnetization and Mössbauer data for single crystal  $\text{Y}_2\text{Fe}_{17}$  reveal an anisotropy of the magnetization, which is associated with the large planar magnetic anisotropy.<sup>25</sup> A large anisotropy of the orbital contribution to the hyperfine field was also deduced from these Mössbauer measurements in large applied magnetic fields. The temperature and field dependence of the hyperfine interactions have been discussed in terms of the individual Fe site moments.<sup>25–27</sup> A pressure-induced phase transition has recently been reported and analyzed in terms of a phenomenological Ginzburg-Landau functional theory.<sup>28</sup>

For confirmation of the calculated local moment variations, reliable microscopic data for the site magnetization in hexagonal  $\text{Y}_2\text{Fe}_{17}$  would appear to be highly desirable for an overall explanation of the magnetism of this important system. In order to obtain experimental data on the distribution of the local-Fe-moment polarized-neutron-diffraction measurements have been performed on a single crystal of hexagonal  $\text{Y}_2\text{Fe}_{17}$ . Exact details of the crystal structure have been obtained from x-ray-diffraction data. This is necessary, since a precise knowledge of the structure is a prerequisite for an accurate determination of the magnetic structure factors measured with neutrons. This is an acute problem in  $R_2\text{Fe}_{17}$  compounds, since it is well known that these materials are very susceptible to partial disordering and form structures, which are a departure from the ordered  $\text{Th}_2\text{Ni}_{17}$  structure. The prime objective was to determine the site dependence of the Fe magnetic moments and, in the presence of structural disorder, to make meaningful comparisons with recent electronic band-structure calculations.

## II. EXPERIMENTAL DETAILS

The single-crystalline  $\text{Y}_2\text{Fe}_{17}$  has been grown in an adapted tri-arc Czochralski apparatus in a purified argon atmosphere at the Material Centre ALMOS of the University of Amsterdam. A water-cooled rotating crucible contains the melt and a pulling rod, rotating in the opposite direction, holds the seed. The melt is heated by three arcs, while, a fourth arc heats a titanium button which serves as a getter. The starting materials (99.9 at. % pure Y and 99.98 at. % pure Fe) were melted together in an almost stoichiometric ratio with only a small excess of Y to compensate the loss due to evaporation. The crystal was pulled out of the melt, during which the diameter of the crystal was controlled by the arc current and the pulling speed of the rod. In this manner a high-quality single crystal was obtained.

The crystallographic structure has been determined at room temperature by x-ray diffraction using a Philips PW 1100 single-crystal diffractometer and Mo  $K\alpha$  wavelength radiation at the Centro di Strutturistica Diffratometrica of the University of Parma. A cylindrically

shaped crystal of approximately  $0.005 \text{ mm}^3$  was used for this purpose. A total of 553 observed reflections, with integrated intensities  $I > 3\sigma(I)$ , were measured in a quadrant of reciprocal space. When corrected for Lorentz and polarization effects these were merged, after absorption corrections<sup>29</sup> and averaging of symmetry related reflections, into 134 unique structure factors utilized for refinement of the structure.

The polarized-neutron-diffraction measurements were made on a single crystal of about  $9 \text{ mm}^3$  in volume using the 5C1 diffractometer at the Laboratoire Léon Brillouin, Centre d'Etudes Nucléaires de Saclay, France. The sample was supported at the center of an asymmetric split-coil superconducting magnet so that the  $b$  axis was approximately parallel to the  $\omega$  axis of the diffractometer and to the applied magnetic field. The instrument is fitted with a detector that can be tilted out of the horizontal plane to allow reflections with scattering vectors out of the horizontal plane to be measured in normal beam geometry. A FeCo single crystal was used to select neutrons with wavelength of  $0.84 \text{ \AA}$  and to polarize the incident beam (polarization efficiency of 0.96). Suitable filters were used to reduce the  $\frac{\lambda}{2}$  contamination. A Meissner-Majorana cryoflipper, with almost 100% efficiency, was used to invert the neutron polarization. All data were taken at a temperature of 10 K in an applied magnetic field of 5 T; under these conditions, the sample magnetization is saturated along the crystallographic  $b$  axis, which is the easy magnetization direction.

If any part of the magnetization has the periodicity of the nuclear structure, then a contribution to the measured intensity comes from the interference between nuclear and magnetic scattering. This contribution is positive or negative depending on the polarization of the neutron spin relative to the sample magnetization. The experiment consisted of measuring, for a number of Bragg reflections, the flipping ratios  $R = I_+/I_-$ , i.e., the ratio between the peak intensities with neutrons polarized parallel ( $I_+$ ) or antiparallel ( $I_-$ ) to the applied magnetic field.

For a centrosymmetric structure, the measured values of  $R$  lead directly to the ratio between the magnetic and the nuclear structure factors,  $F_M$  and  $F_N$ , which are the Fourier components of the magnetization density and of the density of atomic nuclei in the unit cell, respectively. If the crystallographic structure is known the magnetic structure factors can then be determined in amplitude and phase. About 70 independent  $F_M(hkl)$  have been derived in this way, each one from the average of the flipping ratios measured for at least three equivalent reflections; the typical measuring time was 1 h per flipping ratio.

## III. RESULTS AND DATA ANALYSIS

### A. Single crystal x-ray-diffraction analysis

Given the good contrast in the x-ray-scattering amplitudes between Y and Fe, the crystal structure, and, in particular, any presence of disorder of the ideal  $\text{Th}_2\text{Ni}_{17}$  structure, can be accurately determined. All measured

reflections were indexed in the hexagonal space group  $P6_3/mmc$ , with lattice parameters at room temperature,  $a=8.4620(5)$  Å and  $c=8.2900(5)$  Å, which were refined by a least-squares fitting of the setting angles of 25 selected reflections.

Following earlier studies of this and similar systems, such as  $Ce_2Fe_{17}$ ,<sup>30</sup>  $Lu_2Fe_{17}$ ,<sup>31</sup> and  $Ho_2Fe_{17}$ ,<sup>32</sup> the analysis of the crystal structure was carried out starting from the atomic positions of the ordered  $Th_2Ni_{17}$  type,<sup>1</sup> by taking into account the possibility of a disordered variant that was previously observed for  $Y_2Fe_{18.92}$ .<sup>25</sup> As shown in Fig. 1, in the  $Th_2Ni_{17}$  structure, Th atoms should be on the (2b) and (2d) sites, with Ni atoms on (4f), (6g), (12j), and (12k) positions. When this ordered model was utilized for the structure refinement important residual peaks in the difference Fourier maps clearly indicated the presence of disorder. In particular, dumbbell Fe sites (4e) are formed around the (2b) Y site, whereas an additional Y site (2c) was found to center the (4f) dumbbell. At the same time the (12j) Fe site was found to be split in two. Refinement of the structure was consequently performed on this variant in which disorder occurs entirely in the  $z = 1/4$  plane. The final agreement factor between observed and calculated structure factors was  $R=4\%$  for 117 unique reflections. The refined parameters are reported in Table I and are in good overall agreement with previous structural studies of the  $Y_2Fe_{17}$  system.<sup>25</sup> The refined occupancies for the disordered sites suggests some important considerations. At first the deduced composition of the analyzed crystal is  $Y_2Fe_{17.3}$ , close to the ideal one, in agreement with the results of an electron microprobe analysis performed on the same sample. Moreover, the occupancies of disordered Fe dumbbell and Y sites are correlated with those of the two split Fe (12j) sites, suggesting two possible configurations of the  $z = 1/4$  plane (Fig. 2) in the structure. These configurations produce satisfactory coordinations around Y and Fe dumbbell sites, which are normally observed in these type of structures. The presence of Fe (4e) dumbbells implies that they cannot occur in adjacent layers, in which they would be superimposed along the  $c$  direction, with too short Fe-Fe distances between different Fe dumbbells. Consequently, either these sites are partially vacant (in contrast with their refined occupancy and with the global stoichiometry), or they can occur only in alternate layers.

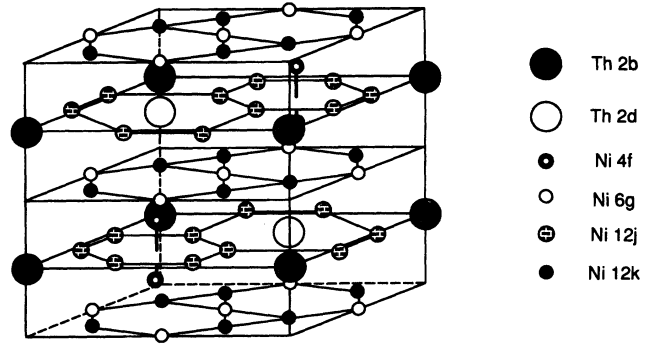


FIG. 1. The ordered crystal structure of  $Th_2Ni_{17}$  type.

All these considerations suggest that the observed disorder could derive from stacking faults consisting of shifts of the hexagonal cell in the  $ab$  plane along the (110) direction. This may be regarded, from a different point of view, as insertion of a rhombohedral sequence along the stacking direction. A schematic representation of the phenomenon, illustrating one of the possible examples, is shown in Fig. 3. A proposed alternative model would allow for adjustment of the Fe dumbbells at two sites in a layer rather than the single layer. This model would incidentally accommodate a broader range of stoichiometry, which is observed in this system. Use of a single crystal gives a more regular stacking sequence and a more stoichiometric compound in contrast with powder specimens. High-resolution neutron-powder-diffraction measurements on a series of more defective compounds, which might also reveal subtle line broadening effects, would be crucial for refinement of a structural model, which could accommodate the entire phase diagram.

### B. Polarized-neutron-diffraction analysis

For a centrosymmetric structure, both  $F_N$  and  $F_M$  are real, and the flipping ratio is given by

$$R = \frac{F_N^2 + 2pq^2 F_N F_M + q^2 F_M^2}{F_N^2 - 2pq^2 F_N F_M + q^2 F_M^2}, \quad (1)$$

where  $p$  is the neutron polarization and the coefficient  $q$

TABLE I. Refined structural and occupancy factors for  $Y_2Fe_{17.3}$  at 293 K.

Atom	Site	Symmetry	$x$	$y$	$z$	$B$ (Å <sup>2</sup> )	Occupancy(%)
Y <sub>1</sub>	2b	$\bar{6}m2$	0	0	1/4	0.73(23)	77(3)
Fe <sub>1</sub>	4e	$3m$	0	0	0.403(6)	0.79(21)	23(3)
Y <sub>2</sub>	2d	$\bar{6}m2$	1/3	2/3	3/4	0.70(11)	100
Y <sub>3</sub>	2c	$\bar{6}m2$	1/3	2/3	1/4	0.79(17)	20(3)
Fe <sub>2</sub>	4f	$3m$	1/3	2/3	0.105(1)	0.39(13)	80(3)
Fe <sub>3</sub>	6g	$2/m$	1/2	0	0	0.27(6)	100
Fe <sub>4a</sub>	12j	$3m$	0.327(3)	0.374(2)	1/4	0.49(9)	71(3)
Fe <sub>4b</sub>	12j	$3m$	0.297(4)	0.296(4)	1/4	0.49(9)	29(3)
Fe <sub>5</sub>	12k	$3m$	0.169(1)	0.337(2)	0.487(7)	0.69(14)	100

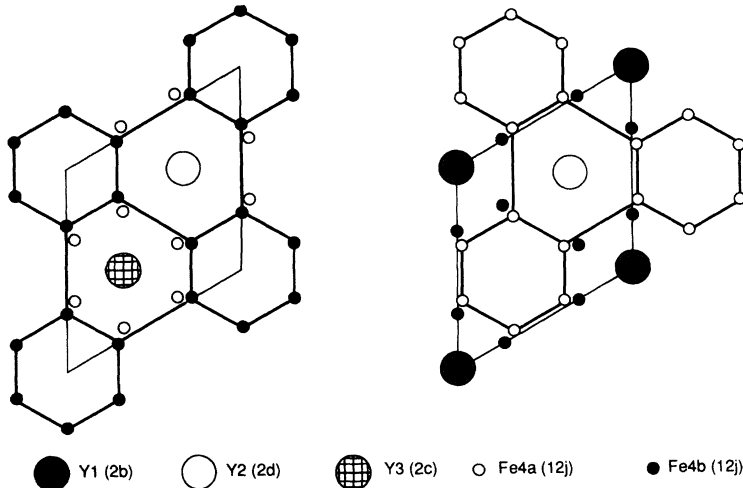


FIG. 2. Possible configurations of the  $z=1/4$  plane resulting from the refined site occupancies of  $Y_2Fe_{17}$ .

is equal to  $\sin\alpha$ ,  $\alpha$  being the angle between the magnetic moment direction and the scattering vector  $\mathbf{Q}$  ( $\mathbf{Q}=4\pi\sin\theta/\lambda$  with  $2\theta$  the Bragg angle). The ratio  $\gamma$  between the magnetic and the nuclear structure factors can then be obtained as

$$\gamma = \frac{p \sin\alpha(1+R) \pm \sqrt{p^2 \sin^2\alpha(1+R)^2 - (R-1)^2}}{(R-1) \sin\alpha} \quad (2)$$

from which  $F_M$  can be determined if  $F_N$  is known. The calculation of the nuclear structure factors was performed on the basis of the x-ray-crystallographic refinement, using the parameters reported in Table I, and the values  $b_{Fe} = 9.45 \times 10^{-12}$  cm and  $b_Y = 7.75 \times 10^{-12}$  cm for the respective neutron-nuclear-scattering lengths.

For technical reasons, imposed by the instrument configuration, data have been collected at one incident wavelength only, and it was not possible to check directly the extent of extinction effects through the wavelength dependence of the experimental  $R$  values. Unpolarized-neutron diffraction was therefore used to measure for a

number of weak, medium, and strong reflections, the integrated intensity  $I$ ,

$$I = kF_N^2(1+q^2\gamma^2)A(\theta,\mu), \quad (3)$$

where  $k$  is an instrumental constant and  $A(\theta,\mu)$  is the absorption factor applicable for a sphere (an absorption coefficient  $\mu = 8.46 \times 10^{-2}$  cm $^{-1}$  was used). Experimental values of  $F_N$  have then been extracted from these measurements and compared with the calculated ones. As shown in Fig. 4, the largest intensity loss, due to extinction, is of the order 10% for the strongest reflections. These have been omitted in the analysis of the polarized neutron data. For medium and weak reflections the extinction effects can be neglected.

The projection of the magnetization density, in the plane perpendicular to the crystallographic  $b^*$  axis, was obtained by carrying out a Fourier sum of the magnetic structure factors for  $(hkl)$  reflections with  $k=0$ . In order to reduce series termination errors the results were averaged over a cube of edge  $\delta = 0.5$  Å centered at the point  $(x,y,z)$ . The average Fourier map so obtained is shown in Fig. 5. Contour levels are drawn from  $-0.7$  to

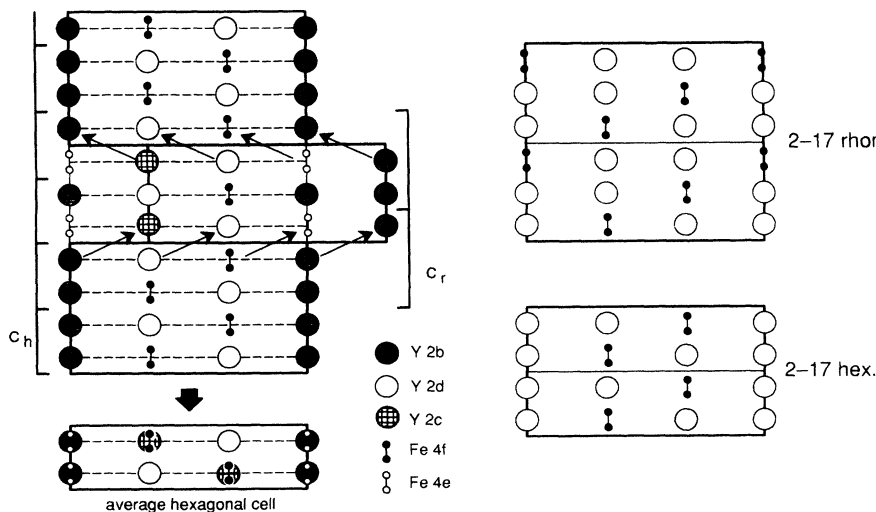


FIG. 3. Schematic representation (view along 110) of a stacking fault mechanism leading to structural disorder in the hexagonal cell as observed from the experimental x-ray-diffraction data for  $Y_2Fe_{17}$ .

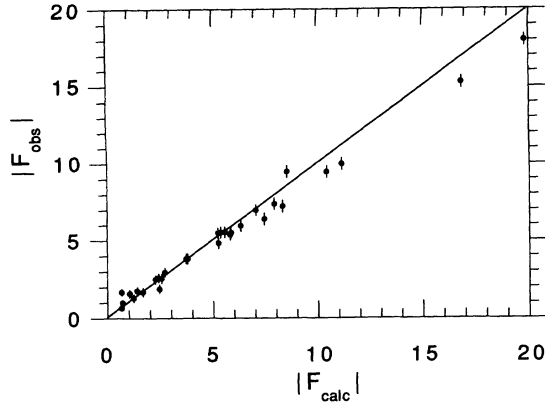


FIG. 4. Plot of observed vs calculated nuclear structure factors. The solid line has a slope equal to unity. For weak and medium reflections, the reduction of intensity due to extinction is negligible.

$3.2 \mu_B \text{ \AA}^{-2}$  with an interval of  $0.5 \mu_B \text{ \AA}^{-2}$ . No contour is drawn at zero. A level of  $\pm 1$  contour is barely significant corresponding, approximatively, to twice the experimental standard deviation. It must be noted that, besides being affected by truncation errors, the map shown in Fig. 5 also suffers from the absence of  $F_M$  terms associated with large  $(hkl)$  values, which were not measured because the corresponding nuclear structure factors  $F_N$  were too large. This introduces distortions that are difficult to correct.

The refinement of the magnetic moments on the different sites was performed by using a least-squares routine based on a multipolar expansion of the spin density.<sup>33-35</sup> The magnetic structure factors are written as

$$F_M(\mathbf{Q}) = \sum_j \left( \sum_{l=0}^{\infty} \Phi_l^j(\mathbf{Q}) \sum_{m=-1}^{m=1} P_{lm}^j Y_{lm}^j(\theta, \phi) \right) \times e^{i\mathbf{Q} \cdot \mathbf{r}_j} e^{-W_j}, \quad (4)$$

where  $\Phi_l(\mathbf{Q})$  is the Fourier-Bessel transform of the radial part of the wave function,  $Y_{lm}(\theta, \phi)$  are real spherical harmonics,  $W_j$  is the Debye-Waller factor, and the  $P_{lm}^j$  are the parameters to be refined by the least-squares procedure to obtain the best fit to the measured magnetic structure factors. The magnetic moment carried by the atoms is given by the population coefficient  $P_{00}^j$  of the corresponding spherical term. In the present case the available set of experimental data does not allow for reliable modelling of the shape of the spin density and a spherical spin distribution was assumed. For Y and Fe

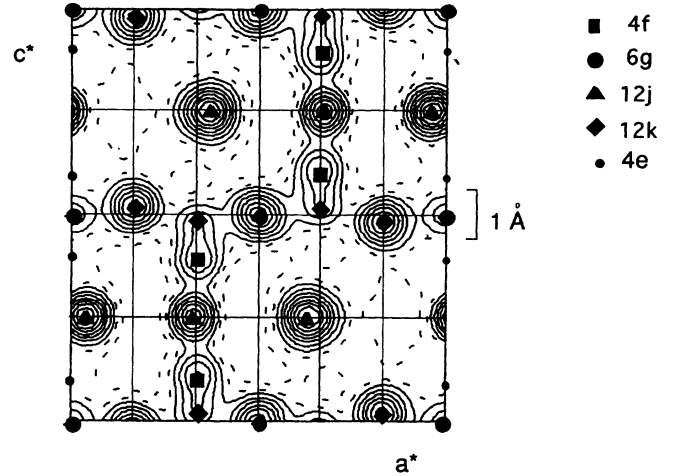


FIG. 5. Projection along the crystallographic  $b^*$  axis of the experimental spin-density obtained as a Fourier synthesis of the magnetic structure factors measured at 10 K for  $\text{Y}_2\text{Fe}_{17}$ . The density is averaged over a cube of edge  $0.5 \text{ \AA}$ . The contour intervals are  $0.5 \mu_B \text{ \AA}^{-2}$ ; negative contours are dashed. No contour is drawn at zero.

the magnetic form factors  $f(Q)$ , measured in their metallic phases, were employed.<sup>36</sup>

Due to the broad spatial distribution of  $4d$  electrons the magnetic form factor for Y is a rapidly decreasing function of the neutron-scattering vector  $Q$ . For this reason, the experiment was not sensitive to the Y magnetic moment, and a fixed value of  $-0.4 \mu_B$  was taken for the refinement. This value has for example also been verified by neutron diffraction for Y in  $\text{Y}_6\text{Fe}_{23}$ .<sup>37</sup> The magnetic moments refined for the Fe atoms are reported in the first column of Table II. The goodness of fit was  $\chi^2=2.16$ , with a weighted agreement factor  $R_w(F)=12\%$ , for 72 magnetic structure factors. The weighting scheme used throughout was always  $1/\sigma^2$ . From these figures the calculated average Fe moment for this sample is  $1.9 \pm 0.1 \mu_B$  at 10 K, which is in good agreement with bulk magnetization measurements reported for the  $\text{Y}_2\text{Fe}_{17}$  system.

#### IV. DISCUSSION

The crystal structure reported here for  $\text{Y}_2\text{Fe}_{17}$  is very similar to that reported for other disordered isomorphous compounds which have the  $\text{Th}_2\text{Ni}_{17}$  structure. The interpretation of the observed disorder, as being due to shifts of the hexagonal cell in the  $ab$  plane due to stacking faults, is not dissimilar to a model of lattice defects

TABLE II. Refined moments for  $\text{Y}_2\text{Fe}_{17.3}$  at 10K. Displayed also are results of recent band-structure calculations and results on  $\text{Y}_2\text{Fe}_{17}$ .

Atom	Site	Population ( $\mu_B$ )	Ref. 10	Ref. 11	Ref. 15
Y <sub>1</sub>	2b	-0.4			
Fe <sub>1</sub>	4e	1.2(0.4)			
Fe <sub>2</sub>	4f	2.5(0.2)	2.31	2.45	2.41
Fe <sub>3</sub>	6g	1.1(0.2)	1.55	2.15	1.91
Fe <sub>4a,4b</sub>	12j	1.83(0.05)	1.86	2.09	2.35
Fe <sub>5</sub>	12k	2.3(0.1)	1.79	2.10	2.12

due to random stacking between sheets of dumbbell Fe atoms and Y atoms for  $Y_2Fe_{17}C_x$  compounds.<sup>38</sup>

The magnetic properties of intermetallic compounds of rare-earth transition metals and, in particular those of  $Y_2Fe_{17}$  compounds, have been treated both in terms of advanced electronic band structure calculations and phenomenological treatments based on mean-field-theory.<sup>39,40</sup> Band-structure treatments can be broadly divided into non-self-consistent and fully self-consistent computations. Non-self-consistent calculations, such as the recursion method within a tight-binding *d*-band model,<sup>10–12,16,17,41</sup> and fully self-consistent calculations based on augmented spherical wave *ab initio* and the local-spin-density approximation, have been carried out and can account for the magnetovolume effect observed for this system.<sup>14,15</sup> A calculation using spin fluctuation theory is also reported and gives a reasonable estimate of the anomalously low Curie point for this system.<sup>13</sup> The available results reported for hexagonal  $Y_2Fe_{17}$  for the site dependence of the local Fe moments are reported in Table II together with the results reported in this paper.

As an overall assessment the magnetic moments obtained in this polarized-neutron-diffraction study are in broad agreement with the available band-structure calculations. In particular, the enhanced moment at the 4*f* site is in good accord with calculations. The band structure calculations, however, have been performed only for the ordered  $Th_2Ni_{17}$  structure. A small calculated orbital moment on 6*g* and 12*k* Fe sites has been suggested as being responsible for the basal plane anisotropy observed in this system.<sup>16</sup> In all cases a large total moment is calculated at the 4*f* site in good agreement with the observed 4*f*-site magnetic moment. This site also possesses the largest calculated orbital contribution. The moment at the 6*g* site is anomalously low and might sug-

gest an antiferromagnetic interaction at this particular site. It has, however, been proposed that the large pressure dependence of the Curie point, as well as the low Curie point, are in fact due to the presence of antiferromagnetic interactions between Fe dumbbell sites.<sup>42</sup> The large error for the calculated moment on the 4*e* dumbbell site is due to the lower sensitivity of the measurement for this site, since the Fe population is low. The results reported here should provide a clearer picture of the magnetic state of Y-Fe intermetallics but electronic structure calculations for the disordered structure, if they can be performed, are most likely required for a more detailed comparison with the present data. Further polarized-neutron-diffraction measurements on other Y-Fe systems would also enhance the validity of the *ab initio* band-structure computations. Similar measurements on structurally less complex and fully ordered compounds, such as  $YFe_2$ , would also enable the Y moment to be measured with a greater precision.

#### ACKNOWLEDGMENTS

The authors thank the Laboratoire Léon Brillouin for provision of neutron-scattering facilities. The authors also wish to thank W. B. Yelon for extremely useful and constructive suggestions concerning the model proposed here for the structural disorder and for proposing a more general alternative model. This work has been supported by the European Programme on Basic Interactions in Rare-Earth Magnets (Brite Euram Programme No. BREU-3039-89) within its Research and Development Programme No. BREU-0068-C(GDF) and also within the CEAM (Concerted European Action On Magnets) programme.

<sup>1</sup>G. Bouchet, J. LaForest, R. Lemaire, and J. Schweizer, C. R. Acad. Sci. (France) **262**, 1227 (1966).

<sup>2</sup>J. V. Florio, N. C. Baenziger, and R. E. Rundle, Acta Cryst. A **26**, 71 (1970).

<sup>3</sup>K. H. J. Buschow, J. Less-Common Met. **11**, 204 (1966).

<sup>4</sup>K. Strnat, G. Hoffer, and A. E. Ray, IEEE Trans. Magn. **MAG-2**, 489 (1966).

<sup>5</sup>K. Schwarz and P. Mohn, Physica B+C **130B**, 26 (1985).

<sup>6</sup>J. G. M. Armitage, T. Dumelow, R. H. Mitchell, P. C. Riedi, J. S. Abell, P. Mohn, and K. Schwarz, J. Phys. F **16**, L141 (1986).

<sup>7</sup>T. Dumelow, P. C. Riedi, P. Mohn, K. Schwarz, and Y. Yamada, J. Magn. Magn. Mater. **54-57**, 1081 (1986).

<sup>8</sup>J. M. D. Coey and H. Sun, J. Magn. Magn. Mater. **87**, L251 (1990).

<sup>9</sup>H. Sun, J. M. D. Coey, Y. Otani, and D. P. F. Hurley, J. Phys. Condens. Matter **2**, 6465 (1990).

<sup>10</sup>J. Inoue and M. Shimuzu, J. Phys. F **15**, 1511 (1985).

<sup>11</sup>B. Szpunar, W. E. Wallace, and Jerzy Szpunar, Phys. Rev. B. **36**, 3782 (1987).

<sup>12</sup>B. Szpunar, J. Less-Common Met. **127**, 55 (1987).

<sup>13</sup>P. Mohn and E. P. Wohlfarth, J. Phys. F **17**, 2421 (1987).

<sup>14</sup>R. Coehoorn, Phys. Rev. B **39**, 13072 (1989).

<sup>15</sup>T. Beuerle, P. Braun, and M. Fahnle, J. Magn. Magn. Mater. **94**, L11 (1991).

<sup>16</sup>M. Shimuzu and J. Inoue, J. Magn. Magn. Mater. **54-57**, 963 (1987).

<sup>17</sup>M. Shimuzu and J. Inoue, J. Magn. Magn. Mater. **70**, 61 (1987).

<sup>18</sup>J. G. M. Armitage, T. Dumelow, P. C. Riedi, and J. S. Abell, J. Phys. Condens. Matter **1**, 3987 (1989).

<sup>19</sup>A. V. Andreev, A. V. Deryagin, S. M. Zadvorkin, and G. M. Kvashnin, *Fizika Magnitnykh Materialov (Physics of Magnetic Materials)* (Kalinin State University, Kalininograd, 1985), p. 21.

<sup>20</sup>D. Givord and E. du Tremolet de Lacheisserie, IEEE Trans. Magn. **MAG-12**, 31 (1976).

<sup>21</sup>D. Givord and R. Lemaire, IEEE Trans. Magn. **10**, 109 (1974).

<sup>22</sup>M. Hamano, S. Yajima, and H. Umebayashi, IEEE Trans. Magn. **8**, 518 (1972).

<sup>23</sup>R. S. Perkins and H. Nagel, Physica B **80**, 143 (1975).

<sup>24</sup>B. Matthaei, J. J. M. Franse, S. Sinnema, and R. J. Radwanski, J. Phys. (Paris) Colloq. **49**, C8-533 (1988).

<sup>25</sup>M. T. Averbach-Bouchot, R. Chevalier, J. Deportes, B. Kebe, and R. Lemaire, J. Magn. Magn. Mater. **68**, 190

- (1987).
- <sup>26</sup>W. Steiner and R. Haferl, *Phys. Status Solidi* **42**, 739 (1977).
- <sup>27</sup>L. M. Levinson, E. Rosenberg, A. Shaulov, S. Shtrikman, and K. Strnat, *J. Appl. Phys.* **41**, 910 (1970).
- <sup>28</sup>S. A. Nikitin, A. M. Tishin, M. D. Kuzmin, and Yu. I. Spichkin, *Phys. Lett.* **153**, 155 (1991).
- <sup>29</sup>A. C. T. North, D. C. Philips, and F. S. Mathews, *Acta Crystallogr. A* **24**, 351 (1968).
- <sup>30</sup>D. Givord and R. Lemaire, *C. R. Acad. Sci. (France)* **274**, 1166 (1972).
- <sup>31</sup>D. Givord, R. Lemaire, J. M. Moreau, and E. Roudaut, *J. Less-Common Met.* **29**, 361 (1972).
- <sup>32</sup>A. Norlund Christensen and R. G. Hazell, *Acta Chem. Scandinavica A* **34**, 455 (1980).
- <sup>33</sup>R. F. Stewart, *J. Chem. Phys.* **58**, 1668 (1973).
- <sup>34</sup>P. J. Brown, A. Capiomont, B. Gillon, and J. Schweizer, *J. Magn. Magn. Mater.* **14**, 289 (1979).
- <sup>35</sup>P. Warren, J. B. Forsyth, G. J. McIntyre, and N. Bernhoeft, *J. Phys. Condens. Matter.* **4**, 5795 (1992).
- <sup>36</sup>E. J. Lisher and J. B. Forsyth, *Acta Cryst. A* **27**, 545 (1971).
- <sup>37</sup>K. Hardman, J. J. Rhyne, and W. J. James, *J. Appl. Phys.* **52**, 2049 (1981).
- <sup>38</sup>W. Coene, F. Hakkens, T. H. Jacobs, D. B. de Mooij, and K. H. J. Buschow, *J. Less-Common Met.* **157**, 255 (1990).
- <sup>39</sup>J. Pszczola and K. Krop, *J. Magn. Magn. Mater.* **59**, 95 (1986).
- <sup>40</sup>R. J. Radwanski, *Z. Phys. B* **65**, 65 (1986).
- <sup>41</sup>H. Yamada, J. Inoue, K. Terao, S. Kanda, and M. Shimuzu, *J. Phys. F* **14**, 1943 (1984).
- <sup>42</sup>P. C. M. Gubbens, J. H. F. van Apeldoorn, A. M. van der Kraan, and K. H. J. Buschow, *J. Phys. F* **4**, 921 (1974).

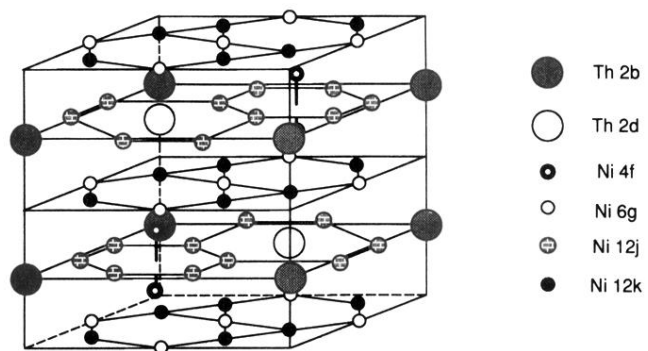


FIG. 1. The ordered crystal structure of  $\text{Th}_2\text{Ni}_{17}$  type.



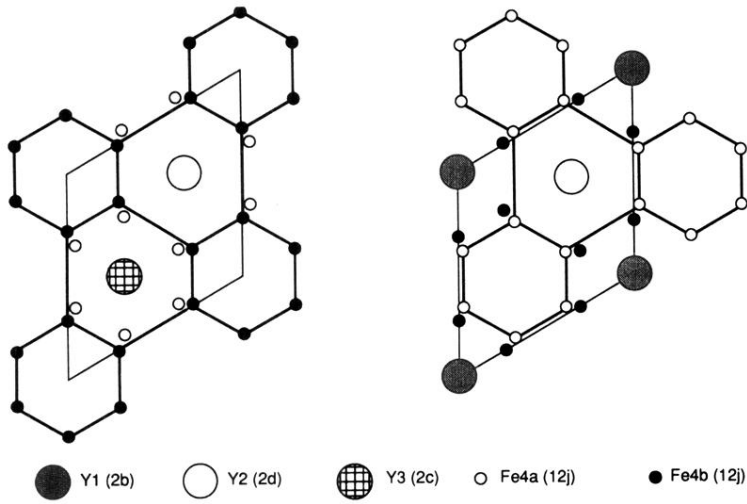


FIG. 2. Possible configurations of the  $z=1/4$  plane resulting from the refined site occupancies of  $Y_2Fe_{17}$ .

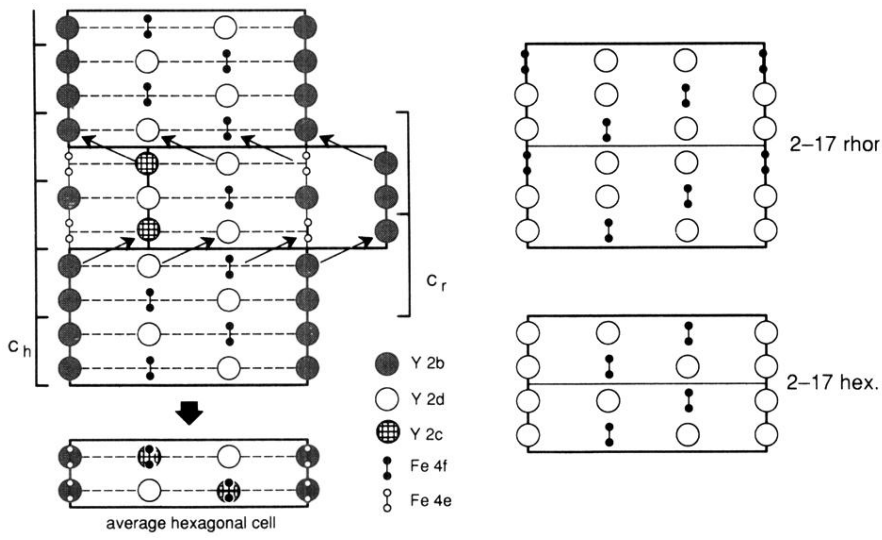


FIG. 3. Schematic representation (view along 110) of a stacking fault mechanism leading to structural disorder in the hexagonal cell as observed from the experimental x-ray-diffraction data for  $Y_2Fe_{17}$ .